diversity

MDPI

Article

Palynological Record of the Aalenian–Bajocian Cooling Event from the Santanghu Basin, Northwest China

Bing Yang, Xinzhi Zhang, Weitong Li, Siyuan Sun and Jinjun Yi *

Cores and Samples Center of Natural Resources, Langfang 065201, China; yangbing0932@126.com (B.Y.); xinzhizcgs@126.com (X.Z.); lwt756651@163.com (W.L.); sunsiyuan1@mail.cgs.gov.cn (S.S.)
* Correspondence: yjinjun@mail.cgs.gov.cn

Abstract: The Aalenian–Bajocian (early Middle Jurassic) cooling event (ABCE) was a significant global climate disturbance during the Jurassic. Our analysis of sporopollen fossils from 18 mudstone and silty mudstone samples, collected from the lacustrine-terrestrial succession Xishanyao Formation in the Santanghu Basin, Northwest China, revealed a total of 191 species belonging to 53 genera. We identified an assemblage, the *Cyathidites–Deltoidospora–Osmundacidites–Cycadopites* assemblage, which dates to the Aalenian–Bajocian (early Middle Jurassic). This assemblage can be further divided into three subassemblages in stratigraphic order: the *Cyathidites–Osmundacidites–Cycadopites* subassemblage, the *Cyathidites–Cycadopites–Psophosphaera* subassemblage, and the *Cyathidites–Deltoidospora–Osmundacidites* subassemblage. We applied the Sporomorph EcoGroup (SEG) model to interpret the paleoclimate features. The sporopollen fossils indicate that the Santanghu Basin underwent a shift in vegetation types, from ground cover vegetation as the dominant form to canopy trees and then back to ground cover vegetation as the primary vegetation during the Aalenian–Bajocian. The SEG model analysis demonstrates that the CCP subassemblage is characterized by a low lowland SEG/upland SEG ratio, low wetter/drier ratio within the lowland SEG, and a low warmer/cooler ratio within the lowland SEG. These characteristics reflect the vegetation's response to the ABCE in the Santanghu Basin.

Keywords: sporopollen fossil; Sporomorph EcoGroup model; vegetation; paleoclimate; Jurassic; Sangtanghu Basin; Northwest China

check for updates

Citation: Yang, B.; Zhang, X.; Li, W.; Sun, S.; Yi, J. Palynological Record of the Aalenian–Bajocian Cooling Event from the Santanghu Basin, Northwest China. *Diversity* **2024**, *16*, 369. https://doi.org/10.3390/d16070369

Academic Editor: Michael Wink

Received: 25 May 2024
Revised: 23 June 2024
Accepted: 24 June 2024
Published: 26 June 2024

Copyright: © 2024 by the authors. Licensee MDPI, Basel, Switzerland. This article is an open access article distributed under the terms and conditions of the Creative Commons Attribution (CC BY) license (https://creativecommons.org/licenses/by/4.0/).

1. Introduction

The Jurassic period holds great significance in the evolutionary history of Earth. During this era, the concentration of CO_2 in the atmosphere was approximately four times higher than today's levels [1], and the average sea surface temperature was roughly 8 °C warmer than the present [2]. The Jurassic has traditionally been viewed as a classic "hothouse" period [3]. However, recent advancements in research precision have led scholars to uncover evidence of several climate fluctuations during the Jurassic and to identify various cooling events [4,5]. The clay mineral composition from the Lower Jurassic in the Paris Basin reveals that sea surface temperatures underwent dramatic fluctuations from the Pliensbachian to the Toarcian [6]. The carbonate carbon and oxygen isotopes, along with major elements from the late Early Jurassic Pliensbachian in the Cleveland Basin, England, suggest the existence of a minor icehouse climate period at that time [7]. Oxygen isotopes in marine invertebrate shells from the northwestern Tethys indicate a significant cooling of Aalenian–Bajocian seawater, with temperature differences reaching up to 10 °C.

Zhang et al. were the first to propose the Aalenian–Bajocian Cooling Event (ABCE) [8]. Globally, the Aalenian–Bajocian witnessed significant cooling, accompanied by a positive drift in organic carbon isotopes [9,10]. This event is reflected in various aspects such as sedimentology, mineralogy, elemental geochemistry, and cyclostratigraphy [8–12].

In northern China, numerous inland basins formed during the Jurassic, with relatively continuous strata that offer prime conditions for studying paleoclimate changes. Palynological evidence from the Yan'an Formation in the Ordos Basin in North China indicates a

warm and humid climate in the subtropical zone during the Middle Jurassic [13]. Studies of plant fossils and palynology suggest that the Middle Jurassic climate in the Minhe Basin in Northwest China was also warm and humid [14]. The Middle Jurassic Xishanyao Formation palynological assemblage from the Tuha Basin in Xinjiang, Northwest China, points to a warm and humid climate with abundant rainfall during the Middle Jurassic [15]. Middle Jurassic sporopollen fossils from the Tarim Basin in southern Xinjiang indicate that the Tarim Basin had a warm and humid climate during the Middle Jurassic [16]. Due to limitations in sample precision, none of the aforementioned studies identified the ABCE.

Plants are highly sensitive to climate change, and vegetation can rapidly replace and migrate in response to climatic shifts [17]. Spores and pollen, as the reproductive organ of plants, serve as an excellent recorder of ancient vegetation and paleoclimate information in sediments. Through palynological fossils, it is possible to restore the vegetation of a study area and reconstruct the paleoclimate and paleoenvironment [18–20].

The Middle Jurassic Xishanyao Formation in the Santanghu Basin, Xinjiang, Northwest China, is a series of coal-bearing strata rich in sporopollen fossils, providing natural materials for studying the Middle Jurassic paleoclimate. This paper presents a systematic paleoclimatological and paleoecological study of palynological samples collected from the Middle Jurassic Xishanyao Formation in the Santanghu Basin, aiming to reconstruct the terrestrial vegetation system and paleoclimate of the Middle Jurassic Santanghu Basin.

2. Geological Setting

The basin stretches in a northwest–southeast direction, covering an area of approximately 2.3×10^4 km^2, in the northeastern part of the Xinjiang Uygur Autonomous Region in Northwest China. The Santanghu Basin was located in the warm temperate humid climate area of northern China in the early Middle Jurassic and away from the ocean [5]. It is an overlapping basin superimposed on the Paleozoic orogenic belt, distinguished by the presence of Permian–Mesozoic and Cenozoic continental sediments. It can be divided into three secondary structural units: the northern uplift zone, the central depression zone, and the southern margin thrust zone [8]. The development and evolution of the Santanghu Basin can be categorized into three main stages: the basement development stage, the development stage of the collision foreland sedimentary basin, and the piedmont basin development stage [21]. During the Late Permian, piedmont depression-type deep lacustrine strata were deposited alongside the uplift of the surrounding mountains. Upon entering the Triassic, the basin experienced a period of overall stable sedimentation [21]. In the Jurassic, influenced by the Indosinian movement, the basin underwent general subsidence, leading to the development of primarily coal-bearing strata of fluvial and lacustrine facies. The Jurassic strata in the Santanghu Basin encompass the Lower Jurassic Badaowan and Sangonghe formations, the Middle Jurassic Xishanyao and Toutunhe formations, and the Upper Jurassic Qigu and Kalazha formations.

The well TYY1 is located 12 km northwest of Santanghu Town, Barkol County, Hami City, Xinjiang, within the southern thrust belt. The main layers are the Lower Jurassic Sangonghe Formation, the Middle Jurassic Xishanyao Formation, and the Toutunhe Formation (Figure 1) in ascending order.

The Xishanyao Formation consists of a sequence of terrigenous clastic rocks, primarily composed of gray-white sandstone, gray-black mudstone, and coal seams and is characterized by the development of braided river delta and lake sedimentary systems.

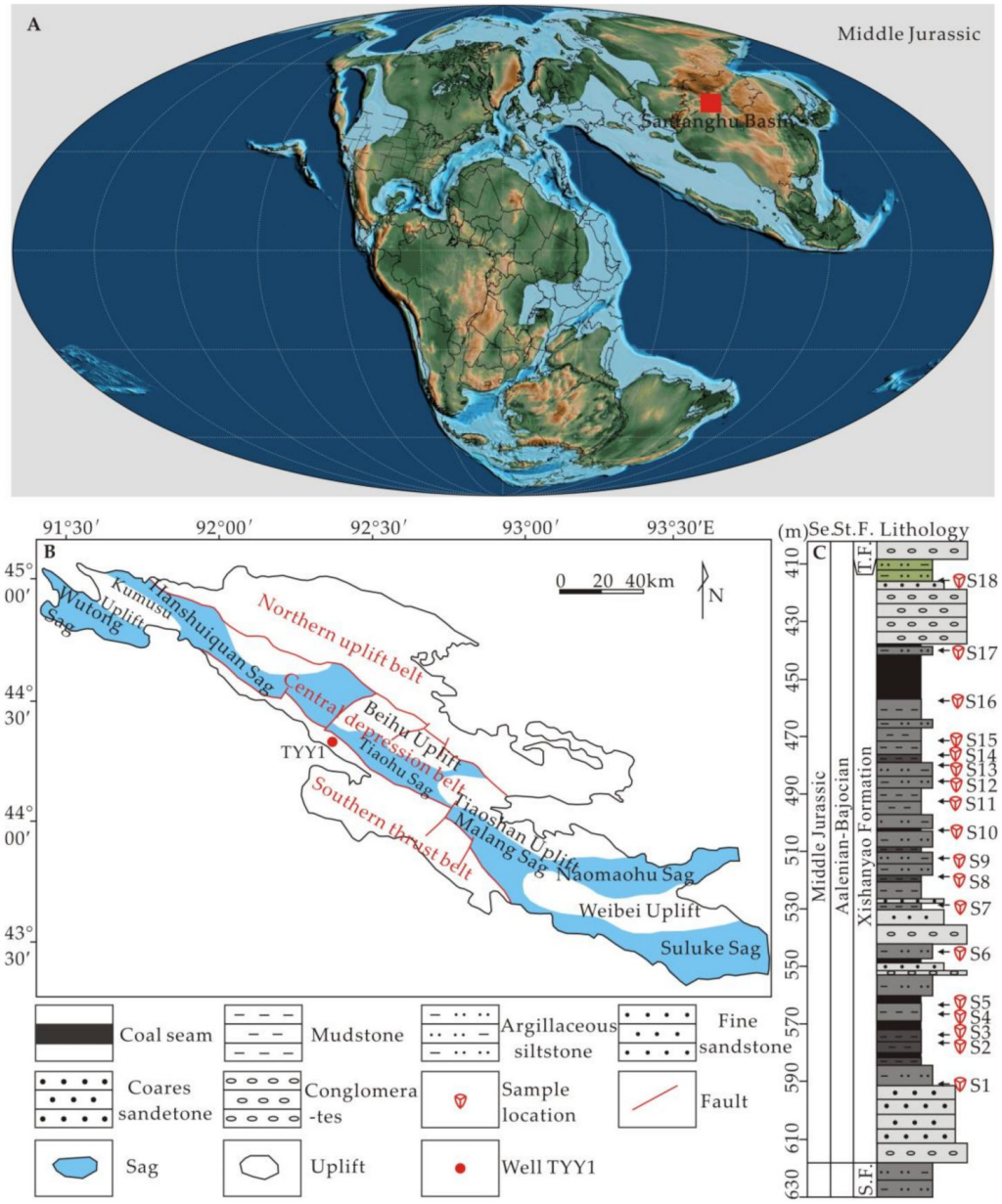


Figure 1. (**A**). Global paleogeographic of Middle Jurassic; (**B**). Geologic map of the Santanghu Basin (modified from the reference [22]); (**C**). Lithological column of the Xishanyao Formation. Se. = Series; St. = Stage; F. = Formation; S.F. = Sangonghe Formation; T.F. = Toutunhe Formation.

3. Materials and Methods

Eighteen palynological samples were collected from mudstone and silty mudstone in the 591.1 m–416.1 m section of Well TYY1. Each 50 g sample was broken into pieces <1.0 mm in diameter and treated with HCl (10%) for 12 h, HF (40%) for 2 days, and HCl (36%) for 12 h. ZnCl-mixed KI heavy liquid (2.2 g/cm^3) was used to gather the palynomorphs. Spore–pollen analysis was performed at the Institute of Geology, Chinese Academy of Geological Sciences. All samples, slides, and stubs, numbered accordingly, were housed in the Cores and Samples Centre of Natural Resources, Langfang, China. The statistical number of sporopollen grains in each sample was greater than 200 grains. Details of the samples are provided in the Supplementary Material. The relative abundance of sporopollen fossils was calculated using Tilia software.3.0.3 The subassemblages were recognized using CONISS within Tilia in ascending order [23,24].

The Sporomorph EcoGroup (SEG) was established by Abbink et al. with the premise that palynomorph assemblages are indicative of the parent plant community [25]. This model infers the existence of ancient ecological communities with distinct habitats during geological periods. The flora within these communities typically share similar ecological characteristics. The coexistence of spores and pollen within these ancient communities reflects the terrestrial plant composition of these ecological communities. The dispersed spore–pollen assemblage type represents the ecological community and provides a detailed paleoecological interpretation of quantitative palynological data [25,26]. Abbink et al. categorized the non-marine Jurassic–Cretaceous palynoflora into six SEG types: upland SEG, lowland SEG, river SEG, pioneer SEG, coastal SEG, and tidally-influenced SEG [25]. Specific details of each SEG type are documented in Abbink et al., Li et al., and Li et al. [25–27].

4. Results

A total of 190 species belonging to 53 genera of spores and pollen were identified in the samples, including bryophyte spores, 1 species in 1 genus; fern spores, 77 species in 26 genera; and gymnosperm pollen, 112 species in 26 genera.

The content of gymnosperm pollen, ranging from 12.8% to 87.6% with an average of 53.5%, was slightly higher than that of fern spores, which ranged from 12.4% to 87.2% with an average of 46.4%. A very small amount of bryophyte fossils was also present, with an average content of less than 0.1%. Among the identified specimens, the fern spores were predominantly represented by *Cyathidites* Couper, 1953 (Cyatheaceae), *Deltoidospora* Miner, 1935, emend. R. Potonié, 1956 (Cyatheaceae), and *Osmundacidites* Couper, 1953 (Osmundacidae), while the gymnosperm pollen was dominated by *Cycadopites* Wodehouse ex Wilson et Webster, 1946. Additionally, nonstriated bisaccate pollen constituted a certain proportion of the findings, which ranged from 1.9% to 36.9% with an average of 17.6%. Based on their morphological characteristics, the assemblage can be named as the *Cyathidites–Deltoidospora–Osmundacidites–Cycadopites* (CDOC) assemblage. This assemblage can be further subdivided into three subassemblies (Figures 2–4).

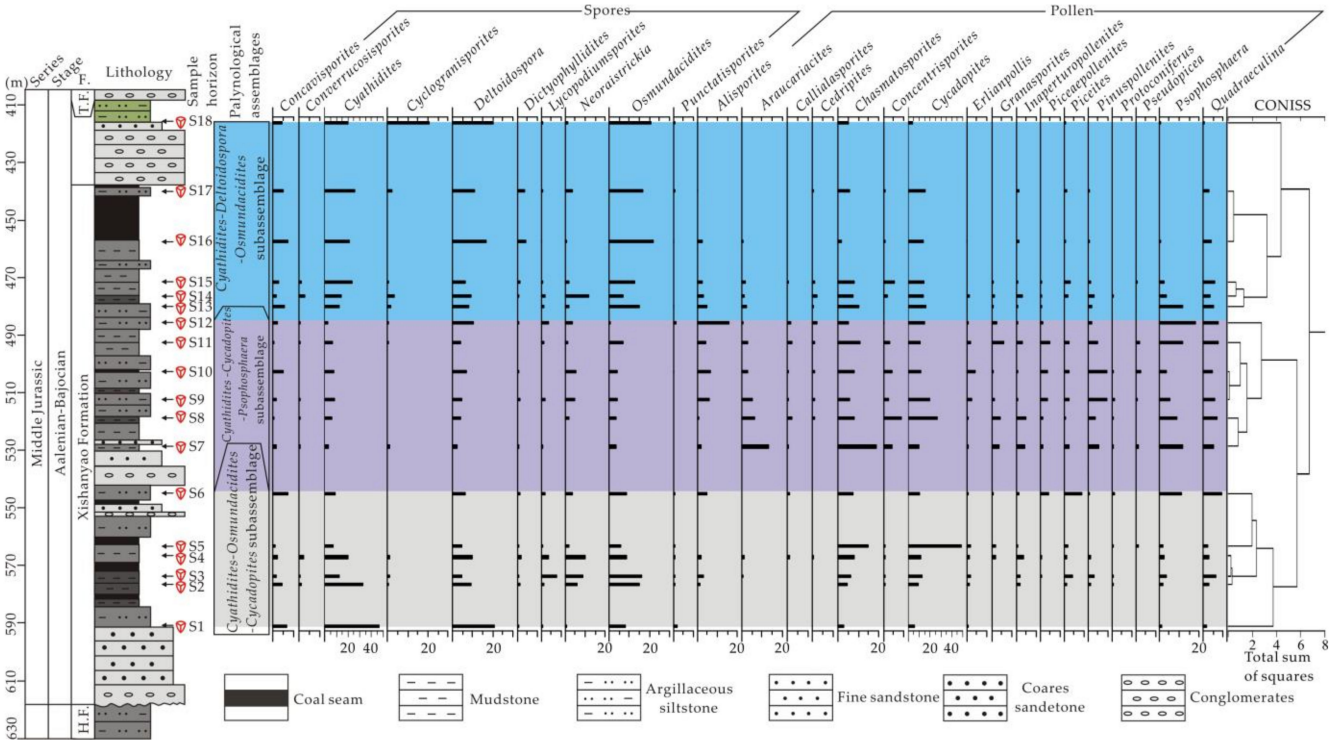


Figure 2. Vertical distribution of major representatives of spore and pollen through the Xishanyao Formation in Well TYY1, Santanghu Basin. Se. = Series; St. = Stage; F. = Formation; S.F. = Sangonghe Formation; T.F. = Toutunhe Formation.

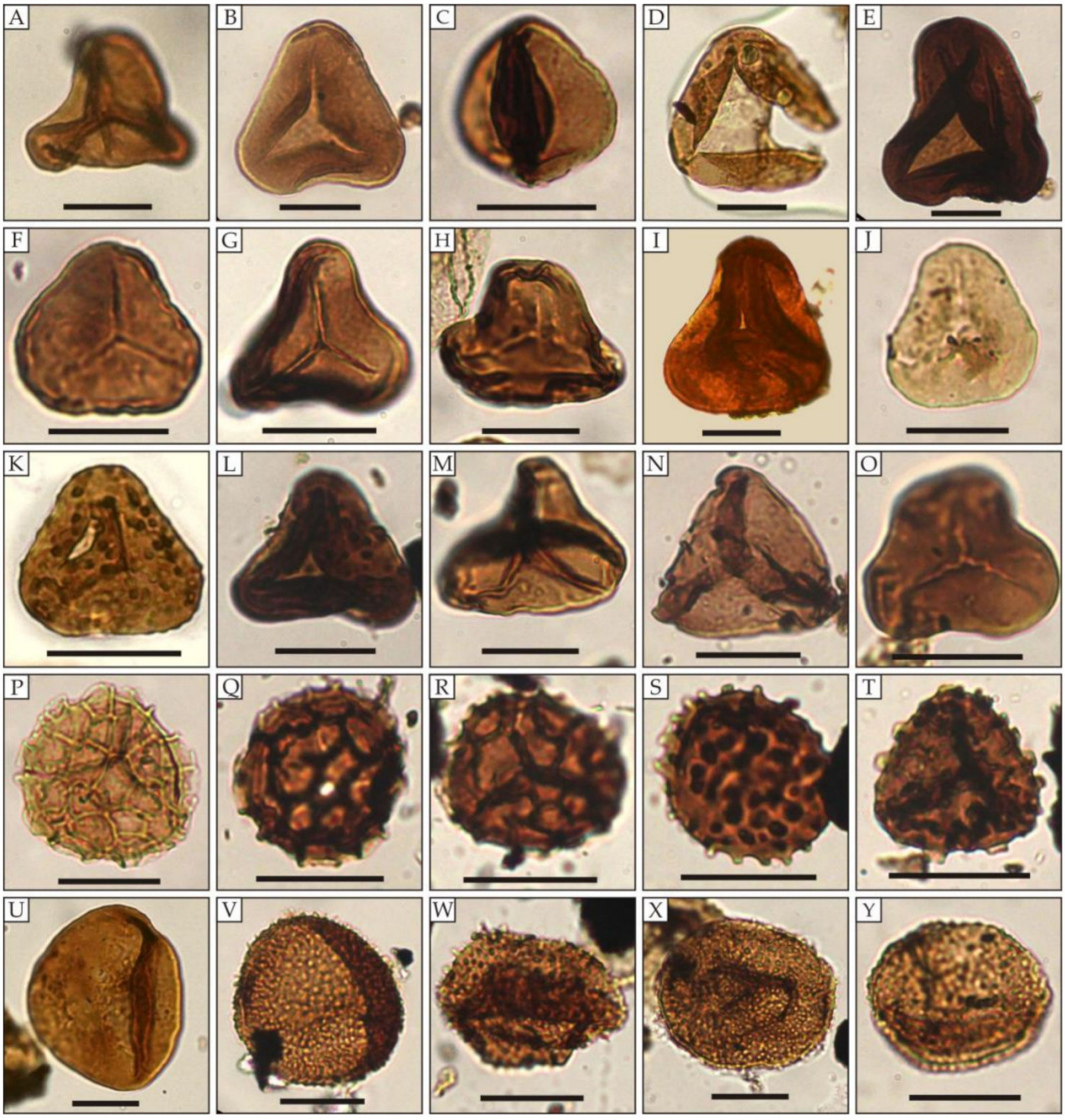


Figure 3. Representatives of spore in the Xishanyao Formation, Santanghu Basin: (**A**) *Concavisporites toralis* (Leschik, 1955) Nilsson, 1958; (**B**) *Cyathidites minor*; (**C**) *Cyathidites trilobayus* San. et Jain, 1964; (**D**) *Cyathidites medicus* San. et Jain, 1964; (**E**) *Cyathidites australis* Couper, 1953; (**F**) *Deltoidospora hallii* Miner, 1935; (**G**) *Deltoidospora plicata* Pu et Wu, 1982; (**H**) *Deltoidospora torosus* Zhang, 1984; (**I**) *Dictyophyllidites mortoni* (De Jersey) Playford et Dettmann, 1965; (**J**) *Dictyophyllidites harrisii* Couper, 1958; (**K**) *Converrucosisporites venitus* Batten, 1973; (**L**) *Converrucosisporites sparsus* Shang, 1981; (**M**) *Alsophilidites arcuatus* (Bolkhovitina) Xu et Zhang, 1980; (**N**) *Auritulinasporites scanicus* Nilsson, 1958; (**O**) *Undulatisporites concavus* Kedves, 1961; (**P**) *Lycopodiumsporites subrotundum* (Kara-Mursa) Pocock, 1970; (**Q**,**R**) *Lycopodiumsporites austroclavatidites* (Cookson) Potonié, 1956; (**S**) *Neoraistrickia minor* Xu et Zhang, 1980; (**T**) *Neoraistrickia gristhorpensis* (Couper) Tralau, 1968; (**U**) *Laevigatosporites ovatus* Wilson et Webster, 1946; (**V**) *Osmundacidites speciosus* (Verb.) Zhang, 1965; (**W**) *Osmundacidites osmundaeformis* (Zhang) Ye, 1981; (**X**) *Osmundacidites senectus* Balme, 1963; (**Y**) *Osmundacidites parvus* De Jersey, 1962. (The scale bar represents 20 μm).

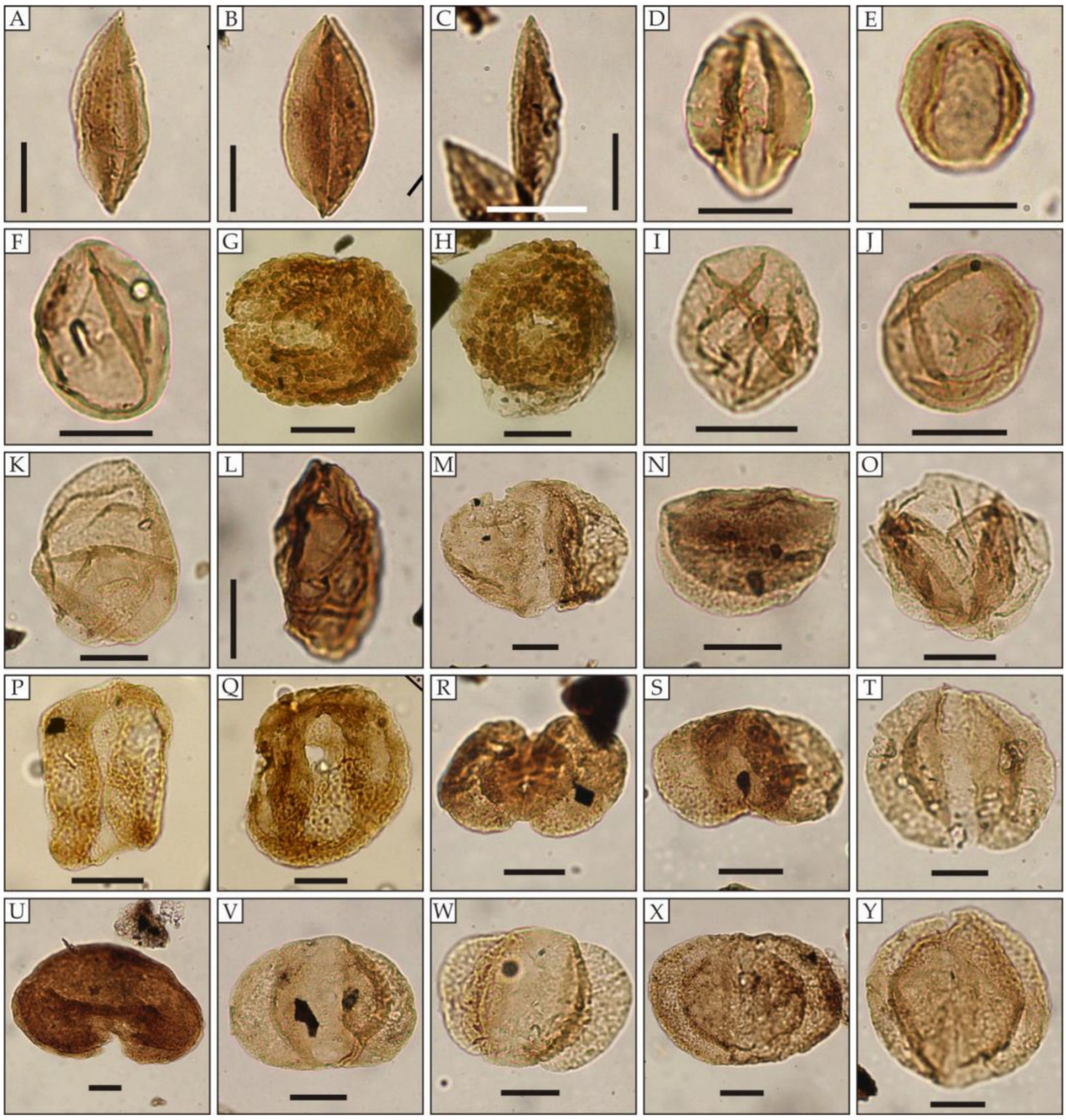


Figure 4. Representatives of pollen in the Xishanyao Formation, Santanghu Basin: (**A**,**B**) *Cycadopites subgranulosus* (Couper) Bharadwaj et Singh, 1964; (**C**) *Cycadopites fusiformis* (Nilsson) Arjang, 1975; (**D**) *Monosulcites minimus* Cookson, 1947; (**E**) *Chasmatosporites elegans* Nilsson, 1958; (**F**) *Chasmatosporites triangularis* Li, Duan et Du, 1982; (**G**) *Cerebropollenites macroverrucosus* (Thierg) Pocock, 1970; (**H**) *Cerebropollenites carlylensis* Pocock, 1970; (**I**) *Inaperturopollenites dubius* (Potonié et Venitz) Thomson et Pflug, 1953; (**J**) *Araucariacites australis* Cookson, 1947; (**K**) *Psophosphaera flavus* (Leschik) Qian, Zhao et Wu, 1983; (**L**) *Psophosphaera undata* (Bolkhovitina) Zhang, 1978; (**M**) *Alisporites australis* De Jersey, 1962; (**N**) *Erlianpollis minisculus* Zhao, 1987; (**O**) *Concentrisporites hallei* (Nilsson) Wall, 1965; (**P**) *Quadraeculina anellaeformis* Maljavkina, 1949; (**Q**) *Quadraeculina canadensis* (Pocock) Zhang, 1978; (**R**) *Podocarpidites multisimus* (Bolkh.) Pocock, 1970; (**S**) *Podocarpidites multicinus* (Bolkh.) Pocock, 1970; (**T**) *Piceites flavidus* Bolkhovitina, 1956; (**U**) *Piceaepollenites multigrumus* (Bolkh.) Xu et Zhang, 1980; (**V**) *Pseudopicea variabiliformis* (Mal.) Bolkhovitina, 1956; (**W**) *Pinuspollenites enodtus* (Bolkh.) Li, 1984; (**X**) *Protopinus subluteus* Bolkhovitina, 1956; (**Y**) *Pityosporites similis* Balme, 1957. (The scale bar represents 20 μm).

4.1. Palynological Assemblage

4.1.1. Cyathidites–Osmundacidites–Cycadopites (COC) Subassemblage

The COC subassemblage was identified in the lower part of the Xishanyao Formation (591.1 m–545.1 m, samples S1 through S6). Within this subassemblage, the content of fern spores ranges from 20.5% to 87.2%, with an average of 54.5%, slightly surpassing that of gymnosperm pollen, which varies from 12.8% to 79.5%, averaging 45.4%. Mosses are present in minimal quantities, with an average content of just 0.1%.

Among the fern spores, *Cyathidites* and *Deltoidospora* (Cyathidaceae) and *Osmundacidites* (Osmundaceae) are particularly abundant and diverse, with *Cyathidites minor* Couper, 1953, showing a notably higher content than other species. Additionally, *Lycopodiumsporites* Thiergart, 1938 (Lycopodium), and *Neoraistrickia* R. Potonié, 1956 (Selaginella), contribute significantly to the assemblage. The COC subassemblage also includes trace amounts of *Auritulinasporites* Nilsson, 1958, *Laevigatosporites* Ibrahim, 1933, *Cyclogranisporites* R. Potonié et Kremp, 1954, *Lycopodiacidites* Couper, 1953, emend. R. Potonié, 1956, *Punctatisporites* Ibrahim, 1933, emend. R. Potonié et Kremp, 1954, *Undulatisporites* Pflug, 1953, *Punctatosporites* Ibrahim, 1933, *Kyrtomisporis* Mädler, 1964, and others.

Colpate pollen from the genera *Cycadopites* and *Chasmatosporites* Nilsson, 1958, emend. Clarke, 1965, are dominant among the gymnosperm pollen. Nonstriate bisaccate pollen is present in a modest proportion, with contents ranging from 2.5% to 30.2%, averaging around 13.7%. The variation in content between samples is considerable, generally increasing from bottom to top, albeit with small percentage contents.

Furthermore, the COC subassemblage contains minor quantities of *Monosulcites* Cookson ex Couper, 1953, *Psophosphaera* Naumova, 1939, ex Ishchenko, 1952, *Granasporites* Alpern, 1959, *Inaperturopollenites* Pflug et Thomson, 1953, *Araucariacites* Cookson, 1947, ex Couper, 1953, *Callialasporites* Sukh Dev, 1961, *Cerebropollenites* Nilsson, 1958, and others.

4.1.2. Cyathidites–Cycadopites–Psophosphaera (CCP) Subassemblage

The CCP subassemblage is recognized in the middle of the Xishanyao Formation (545.1 m–485.6 m, Samples S7 through S12). Among them, gymnosperm pollen is significantly higher than fern spores, with pollen content ranging from 70.3% to 87.6%, and an average content of 77.5%. The spore content ranges from 12.4% to 29.7%, with an average content of 22.4%. There are very few mosses, with an average content of only 0.1%. Among them, the content of the genus *Cyathidites* in fern spores is relatively high, but it does not form a dominant genus. The highest content is only 7.8%. The content of *Cyathidites minor* is relatively high in this genus. In addition, the content of *Osmundacidites* and *Deltoidospora* is slightly lower than that of *Cyathidites*, and spores of other genera appear rarely or sporadically in this subassemblage. The species diversity in gymnosperm pollen is significantly higher than that in the COC subassemblage, in which the colpate pollen *Cycadopites* and *Chasmatosporites* still dominate. Differently, the content of the genus *Psophosphaera* increases significantly, and the content of the genus *Araucariacites* also increases significantly. In addition, the content of nonstriate bisaccate pollen increases significantly, ranging from 13.5% to 36.9%, with an average content of 27.0%. In addition, the three genera *Alisporites* Daugherty, 1941, emend. Jansonius, 1971, *Quadraeculina* Maljavkina, 1949, ex R. Potonié, 1960, and *Pinuspollenites* Raatz, 1938, ex P. Potonié, 1958, are relatively dominant in the nonstriate bisaccate pollen. Other genera are similar to the COC subassemblage.

4.1.3. Cyathidites–Deltoidospora–Osmundacidites (CDO) Subassemblage

The CDO subassemblage was identified in the upper part of the Xishanyao Formation (485.6 m–416.1 m, Samples S13 through S18). In comparison to the CCP subassemblage, the proportions of fern spores and gymnosperm pollen in this subassemblage have shifted notably. Fern spores now outnumber gymnosperm pollen, with contents ranging from 45.5% to 84.8% and averaging 62.0%. Gymnosperm pollen contents vary from 15.2% to 53.7%, with an average of 37.7%. Mosses are present sporadically, with an average content of just 0.3%. The gymnosperm spores in the CDO subassemblage are similar to those in the

CCP subassemblage, primarily consisting of *Cyathidites* and *Deltoidospora* (Cyathidaceae) and *Osmundacidites* (Osmundaceae). The content of *Cyathidites minor* remains significantly higher than that of other species. However, the contents of Cyathidaceae and Osmundaceae in this subassemblage exceed those in the other two subassemblages. Additionally, the content of *Concavisporites* Pflug, 1953, emend. Delcourt et Sprumont, 1955, has increased substantially. Among the gymnosperm pollen, the colpate pollen genera *Cycadopites* and *Chasmatosporites* retain their dominance, though their content has diminished slightly compared to the CCP subassemblage. The nonstriate bisaccate pollen content in the CDO subassemblage has decreased markedly, ranging from 1.9% to 16.7% with an average of 10.2%, generally showing a declining trend from bottom to top. Within this pollen type, only *Quadraeculina* maintains a relatively high content, while other genera are present in very low amounts.

4.2. Sporomorph EcoGroup Analysis

To classify the SEG types of pollen ecological groups, it is necessary to first establish the relationship between the parent plants corresponding to the spore and pollen fossils through previous research. Then, modern relatives are identified, combined with an examination of their ecological environments, and finally, the main spore and pollen species are classified into ecological types.

Following the classification scheme of Abbink et al., ferns typically thrive in humid and warm environments and are thus classified into the lowland SEG [25]. In this study, families such as Cyatheaceae, Osmundaceae, Dipteridaceae/Matoniaceae, Dicksoniaceae, Pteridaceae, Marattiaceae, and a few genera like *Auritulinasporites* and *Punctatosporites* with unknown affinities belong to this group. Horsetails, extant gymnosperms, are usually found in humid environments and are categorized under the warm and humid lowland SEG. Cycads, another gymnosperm group, are typically classified as inhabiting dry, cool lowland SEG environments. Although Abbink et al. classified Araucariaceae into the coastal SEG [25], Kershaw and Wagstaff argued that since the Triassic, this group has predominantly thrived in rainforest environments under moderate temperature and relatively dry conditions [28]. Thus, it is classified as a dry and warm lowland SEG in this study. Conifers in the Mesozoic generally populated upland forests, hence they are classified as an upland SEG, including families like Pinaceae, Podocarpaceae, and seed ferns. Other conifer genera like *Protopinus* Bolkhovitina, 1952, ex 1956, *Protoconiferus* Bolkhovitina, 1952, ex 1956, *Pseudopicea* Bolkhovitina, 1956, *Pityosporites* Seward, 1914, emend. Manum, 1960, *Erlianpollis* Zhao, 1987, and others may be related to Pinaceae and hence classified into the upland SEG [26]. Lycopodiopsids, according to the geographical distribution of extant species, are often found in the lowland, rivers, or tidal-affected SEGs [25]. However, since the Xishanyao Formation mainly comprises fluvial-lacustrine facies, this study classifies lycopodiopsids into the river SEG. Mosses typically inhabit humid environments near water bodies, thus they are classified into the river SEG. Additionally, *Cerebropollenites* is classified under the pioneer SEG [25]. The botanical affinity and classification of the SEGs in the Xishanyao Formation are summarized in Table 1.

The two primary controlling factors influencing vegetation types as reflected by the SEG model are topography and climate. The most significant topographic factors include sea level fluctuations and tectonic movements. Since the Santanghu Basin is inland, the influence of sea level fluctuations is negligible. Moreover, the Santanghu Basin was relatively stable during the early Middle Jurassic, with minimal tectonic activity and predominantly undergoing erosion [21]. Consequently, the impact of tectonic movements is also minimal. Hence, climate factors emerge as the principal drivers of vegetation type changes in this study. Generally, lowland SEG types are the most susceptible to climate change, while the river SEG and tidal SEG are less affected. The impact of climate on lowland SEG types is evident in the proportion of hygrophytes/xerophytes and the ratio of warmer/cooler elements in the palynomorphs of lowland SEG types. Consequently, paleoclimate evolution and tectonic movements can be quantitatively reconstructed by

delineating the different SEG types of pollen communities and the ratios of lowland SEG wetter/drier elements and warmer/cooler elements.

Table 1. Botanical affinity and classification of the SEGs for dispersed sporomorphs of the Xishanyao Formation in the Santanghu Basin, Xinjiang, China.

Botanical Affinity	Sporomorph Genera	SEG	Ecological Remarks
Ferns (Cyatheaceae)	*Cyathidites*, *Deltoidospora*	Lowland	Wetter, warmer
Ferns (Marattiaceae)	*Cyclogranisporites*		
Ferns (Pteridaceae)	*Asseretospora*		
Ferns (Dipteridaceae/Matoniaceae)	*Dictyophyllidites*, *Concavisporites*		
Ferns (Dipteridaceae)	*Kyrtomisporis*		
Ferns (Dicksoniaceae)	*Converrucosisporites*, *Undulatisporites*, *Leiotriletes*		
Ferns (Osmundaceae)	*Osmundacidites*, *Conbaculatisporites*, *Todisporites*		
Ferns	*Auritulinasporites*		
Horsetails	*Laevigatosporites*, *Calamospora*		
Lycopsids/Horsetails/Marttiaceae	*Punctatisporites*		
Conifers (Taxodiaceae)	*Inaperturopollenites*	Lowland	Wetter, cooler
Conifers (Araucariaceae)	*Psophosphaera*	Lowland	Drier, warmer
Conifers (Araucariaceae)	*Araucariacites*, *Callialasporites*		
Gymnosperms	*Granasporites*	Lowland	Drier, cooler
Cycads/Ginkgophytes	*Chasmatosporites*, *Cycadopites*, *Monosulcites*		
Conifers (Podocarpaceae)	*Podocarpidites*, *Quadraeculina*,	Upland	
Conifers (Pinaceae)	*Cedripites*, *Piceaepollenites*, *Pinuspollenites*, *Piceites*		
Gymnosperms	*Cordaitina*		
Conifers	*Erlianpollis*, *Pityosporites*, *Pseudopinus*, *Pseudopicea*, *Protoconiferus*, *Caytonipollenites*		
Conifers (Pinaceae)/Pteridospermae	*Alisporites*		
Bryophytes	*Alsophilidites*, *Annulispora*, *Sphagnumsporites*	River	
Lycopsids (Lycopodiaceae)	*Lycopodiumsporites*		
Lycopsids (Selaginellaceae)	*Lycopodiacidites*, *Kraeuselisporites*		
Lycopsids (Isoetales)	*Aratrisporites*		
Lycopsids	*Neoraistrickia*, *Densoisporites*		
Conifers (Taxodiaceae)	*Cerebropollenites*	Pioneer	
	Spheripollenties, *Concentrisporites*	Not attributed	

By analyzing the palynological samples from the Santanghu Basin and examining the percentage content of SEGs, the relative abundance of different SEGs of the early Middle Jurassic palynoflora in the basin was determined. Sequence changes, as well as ratios of the lowland SEG/upland SEG, wetter/drier elements ratios in the lowland SEG, and warmer/cooler element ratios in the lowland SEG, were analyzed. Four SEGs were identified in the Xishanyao Formation palynomorph assemblage: the lowland SEG, upland SEG, river SEG, and pioneer SEG. Lowland SEG content predominated, followed by the upland SEG, with the river SEG being relatively minimal, and the pioneer SEG representing very little (Figure 5). The characteristics of each combination are as follows:

COC subassemblage: This subassemblage exhibits a relatively high content of lowland SEG elements, ranging from 61.4% to 95%, with an average of about 77.0%. It generally demonstrates a downward trend from bottom to top. Conversely, the content of upland SEG in this subassemblage is relatively low, ranging from 2.5% to 30.7%, with an average of about 14.4%, and generally increases from bottom to top. The lowland SEG/upland SEG ratio is relatively large, ranging between 2.02 and 38, with a decreasing trend from bottom to top. The wetter/drier element ratio of the lowland SEG is relatively large, ranging from 0.28 to 8.22, with a decreasing trend from bottom to top. Similarly, the warmer/cooler element ratio of the lowland SEG is relatively large, ranging from 0.31 to 9.69, with a decreasing trend from bottom to top. From the evidence presented, it can be inferred that the CDO subassemblage ecological group generally indicates a warm and humid climate environment, gradually transitioning to a dry and cold climate over time.

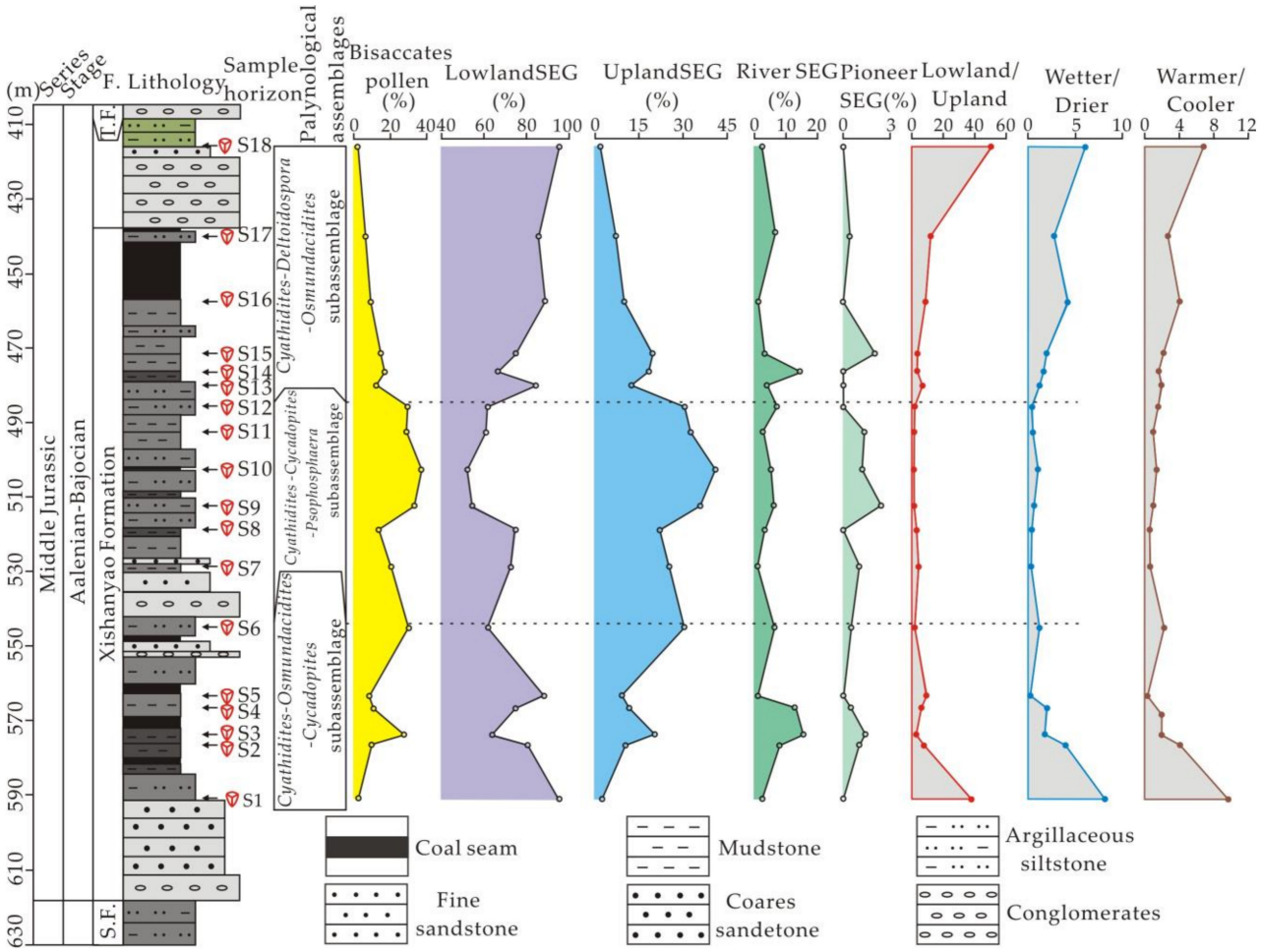


Figure 5. Relative abundances of the SEGs of the Xishanyao Formation in the Santanghu Basin, China.

CCP subassemblage: In comparison to the COC subassemblage, the content of the lowland SEG in this subassemblage is significantly reduced, ranging from 51.9% to 75.1%, with an average of 66.3%. The fluctuation in content remains within a narrow range, indicating stability. Conversely, the upland SEG exhibits a notable increase in abundance, ranging from 21.6% to 40.9%, with an average of 31.0%. The ratio of the lowland SEG/upland SEG is extremely low, between 1.27 and 3.48, with a stable fluctuation pattern. Additionally, both the wetter/drier ratio and the warmer/cooler ratio of the lowland SEG are very low, ranging from 0.27 to 0.95 and from 0.74 to 1.62, respectively. Again, the fluctuations in these ratios are relatively stable. This suggests that the CCP subassemblage ecological group indicates a dry and cold climate environment.

CDO subassemblage: In comparison to the CCP subassemblage, the content of the lowland SEG in this subassemblage has shown a significant increase, ranging from 67.1% to 95.7%, with an average of 82.6%, exhibiting an upward trend from bottom to top. Conversely, the content of the upland SEG has notably decreased, ranging between 1.9% and 19.7%, with an average of 11.7%, showing a declining trend from bottom to top. The lowland SEG/upland SEG ratio is relatively high, ranging between 3.63 and 50.37, with a rising trend from bottom to top. Compared to the lower subassemblage, the wetter/drier element ratio and the warmer/cooler element ratio of the lowland SEG in this assemblage have significantly improved, ranging from 1.04 to 6.2 and from 1.6 to 6.78, respectively, both indicating an upward trend from bottom to top. It is evident that the CDO subassemblage ecological group signifies a warm and humid climate environment, with both temperature and humidity gradually increasing over time.

5. Discussion

5.1. Geological Time

The CDOC assemblage of the Xishanyao Formation is distinguished by the abundance of *Cyathidites* and *Deltoidospora*, both of which are typical genera of the Jurassic period [29,30]. Additionally, there is no typical Triassic genus. However, there are still a small number of remnants of striate bisaccate pollen from the Early Jurassic (such as *Protohaploxypinus* Samoilovichi, 1953, emend. Hart, 1964, *Taeniaesporites* Leschik, 1955, emed. Jansonius, 1962, etc.) and genera like *Cicatricosisporites* R. Potonié et Gelletich, 1933, *Schizaeosporites* R. Potonié ex Delcourt et Sprumont, 1955, and *Trilobosporites* Pant, 1954, and ex R. Potonié, 1956, that were common in the Late Jurassic and Cretaceous. Therefore, it can be generally determined to be a Jurassic assemblage.

Cyathidites minor was widely distributed during the Jurassic and exhibited distinct distribution patterns across different periods. In northern China, the content of this species differed significantly between the Early Jurassic and the Middle Jurassic, with the Middle Jurassic content being notably higher than in the Early Jurassic [31–34]. Consequently, the high content of *Cyathidites minor* is often used as one of the indicators of a Middle Jurassic palynological assemblage [34,35]. The content of this species at the base of the Xishanyao Formation in Well TYY1 in the Santanghu Basin can reach 26.1%, displaying clear characteristics of a Middle Jurassic palynomorph assemblage.

The content of the genus *Neoraistrickia* in the Jurassic of northern China changed with discernible patterns [36]: the content was low in the Early Jurassic, increased in the early Middle Jurassic, and then sharply decreased from the late Middle Jurassic to the Late Jurassic. The highest content of this genus in the CDOC assemblage can reach 11.1%, with high species diversity, consistent with the features of early Middle Jurassic spores and pollen. Moreover, an important species in this genus, *Neoraistrickia gristhorpensis* was first reported in the early Middle Jurassic of Britain [29] and is only found in Middle Jurassic and later. This species is widely distributed in Germany, France, and the Middle Jurassic of Sweden. It can also be found in the Middle Jurassic of northern China, such as in the Yan'an Formation of the Shaanxi–Gansu–Ningxia Basin [37], the Yan'an and Zhiluo Formations in the Chongxin area of Gansu [32], the Zhaogou Formation in the Shiguai Coalfield of Inner Mongolia [31], the third member of the Meiyaogou Formation in the Tuha Basin [33], and the Xishanyao Formation in Shawan County, Xinjiang [38], among others. The genus *Callialasporites* can restrict the maximum age of the deposits, which has its First Appearance Datum (FAD) in the late Pliensbachian [39]. But it tends to proliferate in the Middle Jurassic across worldwide regions. This genus is common in the CDOC assemblage.

Osmundacidites were extremely common in the Middle Jurassic and were often found in certain assemblages during this period. Based on Middle Jurassic sporopollen data from the Junggar Basin and surrounding areas, the genus was relatively abundant in the early Middle Jurassic (Aalenian–Bajocian) and showed a significant decrease in content in the late Middle Jurassic (Bathonian–Callovian). For example, the content of this genus in the Xishanyao Formation of the Honggou section along the Manas River in the Junggar Basin of Xinjiang ranges from 0% to 18.4%, with an average of 6.8%, while in the Toutunhe Formation, it ranges from 1% to 10.5%, averaging 5.4% [40]; the content of this genus in the Middle Jurassic Xishanyao Formation in the Turpan–Shanshan area of Xinjiang is as high as 15.6%, while in the late Middle Jurassic Sanjianfang Formation, it is less than 6.1% [34]; the content of this genus in the Middle Jurassic Xishanyao Formation in the Turpan Depression is as high as 16.1%, while in the late Middle Jurassic Sanjianfang Formation, it is 6.1% [15].

The early Middle Jurassic (Aalenian–Bajocian) sporopollen assemblage in Siberia is characterized by the dominance of *Cyathidites minor* and the presence of abundant *Quadraeculina*, *Neoraistrickia*, *Lycopodiumsporites*, and other genera [41]; the Bajocian palynological assemblage in Yorkshire, UK, is also dominated by *Cyathidites minor* and includes major genera such as *Osmundacidtes*, *Lycopodiumsporites*, *Dictyophyllidites*, *Araucariacites*, and *Classopollis* Pflug, 1953 [29]. All of the above genera, except for *Classopollis*, are major components of the CDOC assemblage.

Furthermore, a large number of *Classopollis* are commonly found in late Middle Jurassic strata in the Junggar Basin and surrounding areas. For instance, the *Classopollis* content in the Middle Jurassic Bathonian Sanjianfang Formation in the Turpan–Hami area ranges from 4.3% to 23.6% [34]; in the Honggou section of Shawan County in the Junggar Basin, the *Classopollis* content of the upper Middle Jurassic Toutunhe Formation ranges from 1.5% to 11.7% [40]; in the Middle Jurassic of the Santanghu Basin, the *Classopollis* content in the upper Toutunhe Formation ranges from 19.2% to 28.2% [42]. The significant increase in *Classopollis* content starting from the Bathonian indicates that the climate of the basin gradually became dry and hot. However, the genus Classopollis is not found in this assemblage, suggesting that the geological age of this assemblage is earlier than the late Middle Jurassic.

Based on the evidence presented above, it can be determined that the geological age of the CDOC assemblage of the Xishanyao Formation in Well TYY1 can be classified as the Aalenian–Bajocian. The plant fossils group named as the *Coniopteris–Raphaelia* assemblage which was discovered in this formation [43], also suggests an Aalenian–Bajocian geological age.

5.2. Paleovegetation Reconstruction

Spores and pollen, as the reproductive organ of plants, provide insight into the plant taxa of the Aalenian–Bajocian period in the Santanghu Basin through the analysis of their parent plants. The plant types of that era mainly included ferns, conifers, cycads, lycopsids, seed ferns, horsetails, and bryophytes, each exhibiting different vegetation features at different times (Figure 6).

COC Period: Ferns dominated the COC ecosystem, with their content ranging from 18.5% to 81.3%, averaging 45.6%. They primarily included families such as Cyatheaceae (*Cyathidites*, *Deltoidospora*), Osmundaceae (*Osmundacidites*, *Todisporites* Couper, 1958, *Conbaculatisporites* Klaus, 1960), Dicksoniaceae (*Leiotriletes* Naumova, 1937, emend. R. Potonié et Kremp, 1954, *Undulatisporites*, *Converrucosisporites* R. Potonié et Kremp, 1954), Dipteridaceae/Matoniaceae (*Kyrtomisporis*, *Dictyophyllidites*, *Concavisporites*), Pteridaceae (*Asseretospora* Schuurman, 1977), Marattiaceae (*Cyclogranispores* R. Potonié et Kremp, 1954), and others. Cyatheaceae and Osmundaceae accounted for the majority of true ferns, with average values of 29.4% and 10.2%, respectively. This type of vegetation formed the main ground cover during this period. Cycads also held a significant position in this ecosystem, with their content varying from 8.9% to 65.5%, averaging 24.0%. They included three genera: *Cycadopites*, *Chasmatosporites*, and *Monosulcites*. This vegetation type constituted the main midstorey during this period. Conifers were less abundant, with their content ranging from 4.0% to 39.1%, averaging 18.2%. They primarily included Pinaceae (*Piceites*, *Pinuspollenites*, *Piceaepollenites*, *Cedripites* Wodehouse, 1933), Podocarpaceae (*Podocarpidites* Cookson ex Couper, 1953, emend. R. Potonié, 1958, *Quadraeculina*), Taxodiaceae (*Cerebropollenites*, *Inaperturopollenites*), Araucariaceae (*Psophosphaera*, *Araucariacites*, *Callialasporites*), and other coniferous trees (*Protopinus*, *Protoconiferus*, *Pseudopicea*, *Pityosporites*, *Erlianpollis*). Pinaceae had a relatively high content among the conifers. This vegetation type formed the main canopy trees of this period. Lycopodiopsids were also relatively common, including genera such as *Lycopodiumsporites*, *Neoraistrickia*, *Aratrisporites*, and *Lycopodiacidites*. Horsetails and seed ferns appeared sporadically in this ecosystem. Overall, the ecosystem of this period was dominated by ground cover vegetation led by ferns, with midstorey vegetation dominated by cycads in a secondary position, and canopy trees dominated by conifers being less abundant.

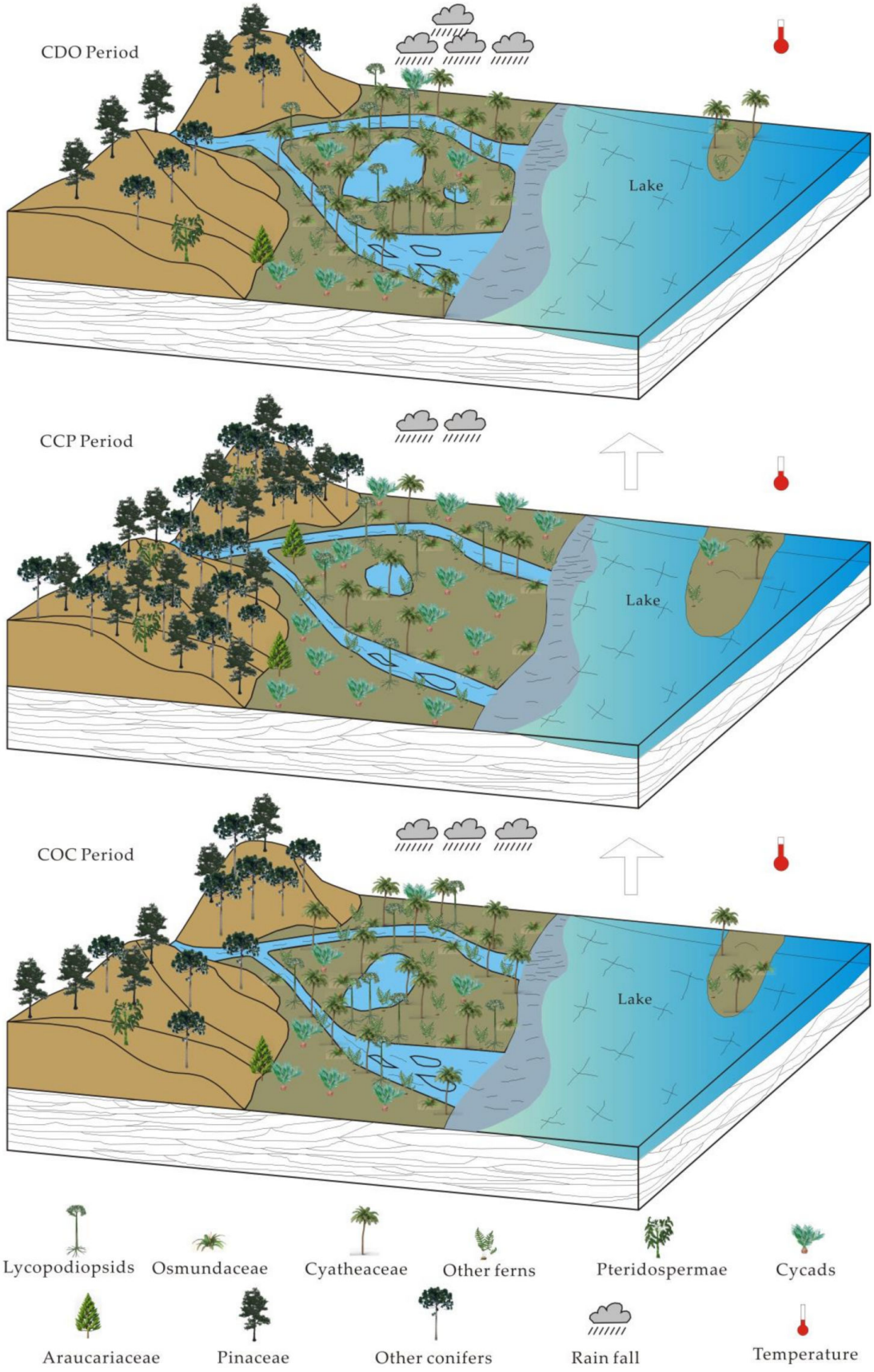


Figure 6. The sketch map of paleoenvironmental and paleovegetation evolution in the early Middle Jurassic Santanghu basin.

CCP Period: In the CCP ecosystem, conifers took over from ferns as the dominant plant type, with their content ranging from 32.8% to 49.1%, averaging 40.1%. They mainly included families such as Pinaceae, Podocarpaceae, Taxodiaceae, Araucariaceae, and other coniferous trees with uncertain affinities. The genus and species categories were generally consistent with those in the COC ecosystem. The content of Pinaceae among the conifers remained high, ranging from 5.6% to 16.1%. Cycads in the CCP ecosystem were second only to conifers, with their content ranging from 19.3% to 35.3%, averaging 24.8%. They included three genera: *Cycadopites*, *Chasmatosporites*, and *Monosulcites*, with *Cycadopites* having the highest content. Compared to the COC ecosystem, ferns were significantly reduced in this ecosystem, with their content ranging from 11.4% to 24.1%, averaging 17.5%. They primarily included families such as Cyatheaceae, Osmundaceae, Dicksoniaceae, Dipteridaceae/Matoniaceae, Pteridaceae, and Marattiaceae. The genus and species categories were generally consistent with those in the COC ecosystem, with the Cyatheaceae family still dominating the ferns, with a content of 5.7% to 14.1%, averaging 10.6%. The content of seed ferns in this ecosystem increased significantly compared to the COC ecosystem. Only the genus *Alisporites* was found in this category, with its content ranging from 0.5% to 15.7%, averaging 5.6%. The content of lycopodiopsids was low in this ecosystem, averaging less than 5%. Additionally, a very small number of horsetails and bryophytes were observed. Generally speaking, the ecosystem of this period was dominated by coniferous trees from families such as Pinaceae, Podocarpaceae, Taxodiaceae, Araucariaceae, and seed ferns. The midstorey vegetation content remained basically unchanged and still occupied a secondary position. The ground cover vegetation dominated by ferns was severely degraded.

CDO Period: During this period, the ecosystem underwent significant changes compared to the CCP ecosystem. Ground cover vegetation dominated by ferns replaced coniferous trees, leading to a significant reduction in canopy trees. The average content of ferns increased from 17.5% in the CCP ecosystem to 56.1%, constituting the main vegetation of the ecosystem during this period. Additionally, a small number of bryophytes and horsetails were observed in the ground cover vegetation. Cycads continued to dominate the midstorey vegetation, with their content ranging from 12.3% to 26.8%, averaging 20.3%. They included three genera: *Cycadopites*, *Chasmatosporites*, and *Monosulcites*. Lycopsids were also common as midstorey vegetation, but their average content was only about 5.0%. The canopy trees were still dominated by Pinaceae, Podocarpaceae, Taxodiaceae, Araucariaceae, and other coniferous trees with uncertain affinities, but their content ranged from 2.8% to 22.1%, averaging only 13.5%. A small amount of seed fern vegetation was also seen among the canopy trees. Overall, the ecosystem of this period was dominated by ground cover vegetation led by ferns, with midstorey vegetation occupying a secondary position, and canopy trees dominated by conifers being severely degraded.

5.3. The Aalenian–Bajocian Cooling Event

Through the SEG model of the Xishanyao Formation, it is evident that the Aalenian–Bajocian climate in the Santanghu Basin underwent a transition from warm and humid conditions to cold and arid conditions, before reverting back to a warm and humid climate. This suggests that the early Middle Jurassic climate in Northwest China was not consistently warm and humid, but rather experienced distinct cooling events during this period, which is uncommon in China. Zhang et al. also observed this phenomenon through elemental geochemistry and clay mineral indicators in the Xishanyao Formation of the Santanghu Basin. These indicators displayed significant negative shifts in both the CIA value and the kaolinite/illite ratio in the central Xishanyao Formation, indicating a response to this cooling event [8]. Additionally, Dai et al. confirmed the occurrence of this cooling event by CIA of mudstone in the Middle Jurassic of the Zigui Basin, South China [12].

Similar cooling events have been documented in the western Tethys Ocean region. For instance, the oxygen isotope records of belemnite fossils and Mg–calcite fossils in the Northwestern Tethys Ocean indicate a significant cooling during the Aalenian–Bajocian period [4,44]. Strontium isotope evidence from British belemnite fossils suggests a negative

drift in $^{87}Sr/^{86}Sr$ during the Bajocian period, indicating a decrease in water temperature [45]. Ferreira et al. analyzed the oxygen isotopes of brachiopod shells in the Middle Jurassic of the Lusitanian Basin in Portugal and found that the $\delta^{18}O$ value increased by 0.5‰ at the Aalenian/Bajocian boundary, corresponding to a temperature drop of 2.5 °C [46]. Bodin et al. investigated the lower Middle Jurassic of the High Atlas Mountains in Morocco and concluded that there was a significant burial of organic carbon at the Aalenian/Bajocian transition, which resulted in a decrease in atmospheric carbon dioxide partial pressure. They estimated that atmospheric carbon dioxide concentration decreased by approximately 120 ppm during this period, speculating on the brief emergence of polar ice caps [47]. These global comparisons highlight the significance of the cooling events observed in the early Middle Jurassic of the Santanghu Basin in this study (Figure 7). It is noteworthy that the cooling event indicated by pollen in this study commenced earlier than previously documented. This discrepancy may stem from imprecise chronological stratigraphy or from the direct and sensitive response of surface vegetation, which lacks the buffering effect of seawater, to environmental fluctuations [48].

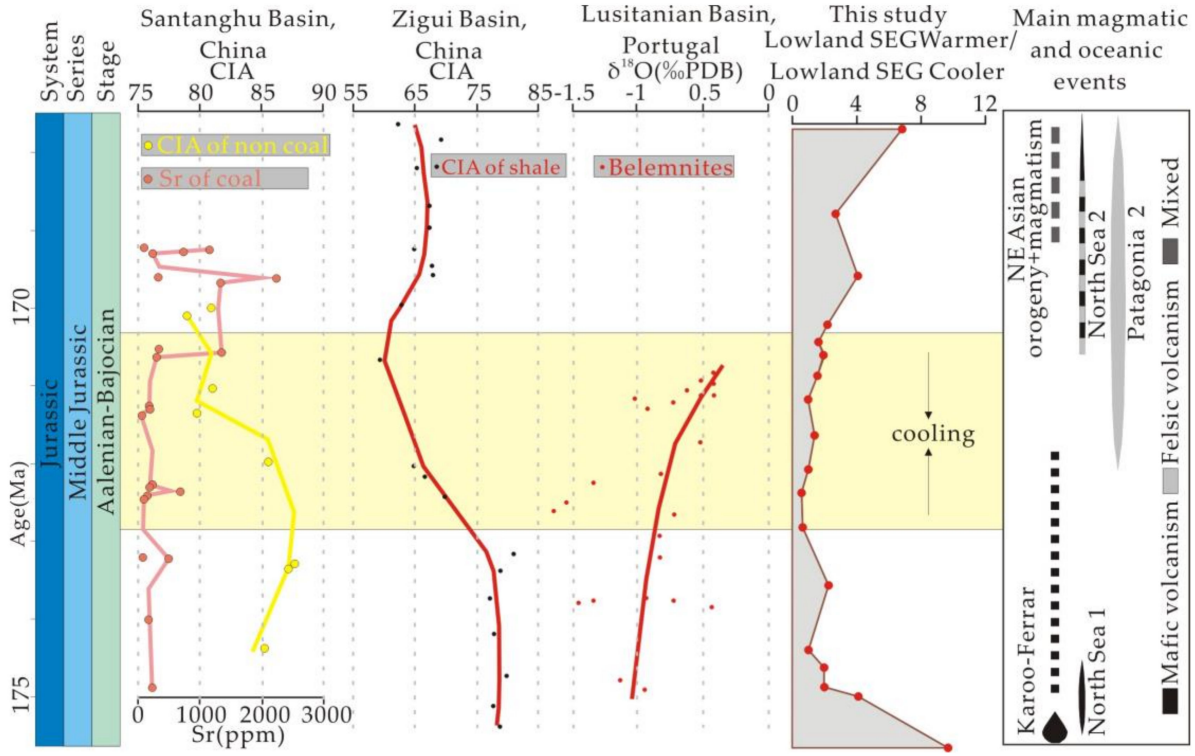


Figure 7. Sporomorph EcoGroup curve compared with the Aalenian–Bajocian Cooling Event. Sr content of coal samples and CIA of non-coal samples are from [8]. CIA data of shales are from [12]. The $\delta^{18}O$ values of belemnites are from [41]. The main magmatic and oceanic events are from [4].

While the cause of the early cooling event in the Middle Jurassic remains a subject of debate, Dera et al. suggested a possible link to a decrease in the partial pressure of atmospheric carbon dioxide, drawing comparisons with significant glacial events throughout the Phanerozoic [4]. It is generally hypothesized that during warm and humid periods, an increased silicate weathering rate enhances the consumption of atmospheric carbon dioxide. Moreover, the accumulation of nutrients and the burial of organic matter further contribute to the reduction in atmospheric carbon dioxide partial pressure [4].

The Karoo–Ferrar large igneous province, which erupted from the Toarcian period and persisted until the Aalenian period, played a significant role in this context. Enhanced water circulation resulting from volcanic events primarily characterized the climate as warm and humid. However, as the large igneous province subsided and atmospheric carbon dioxide was consumed, the greenhouse effect waned [49]. The coldest climate period

observed in this study coincided with the aftermath of the Karoo–Ferrar large igneous province's subsidence. Additionally, the influence of various other significant magmatic activities during the Middle Jurassic, such as the Northeast Asian orogeny, Patagonia magmatic activity Phase 2, and Northern Ocean magmatic activity, cannot be disregarded. The release of carbon dioxide from these events and its subsequent impact on the global climate are noteworthy. The increase in atmospheric carbon dioxide partial pressure due to seafloor baking is known to elevate global temperatures [4]. The cold events during the Aalenian–Bajocian period observed in this study coincide with the intervals of these magmatic events (Figure 7), contributing to the cyclical evolution of the climate during this period—from hot and humid to dry and cold, and then back to hot and humid—as indicated by palynological evidence.

6. Conclusions

We analyzed 18 palynological samples collected from Well TYY1 in the Xishanyao Formation of the Anangu Basin, Xinjiang Uygur Autonomous Region, Northwest China. Through this analysis, we established a sporopollen assemblage, determined the geological age, and reconstructed the ancient vegetation and paleoclimate. Our conclusions are as follows:

(1) The sporopollen assemblage of the Xishanyao Formation is characterized by the *Cyathidites–Deltoidospora–Osmundacidites–Cycadopites* assemblage, dating back to the Aalenian–Bajocian period.

(2) The CDOC assemblage can be further subdivided into three subassemblies: the *Cyathidites–Osmundacidites–Cycadopites* subassemblage; the *Cyathidites–Cycadopites–Psophosphaera* subassemblage; and the *Cyathidites–Deltoidospora–Osmundacidites* subassemblage. During the COC period, the ecosystem was characterized by ground cover vegetation dominated by ferns, midstorey vegetation dominated by cycads with a secondary presence, and upland canopy vegetation dominated by conifers albeit with less abundance. In the CCP period, coniferous trees constituted the main portion of the canopy, while the content of midstorey vegetation remained largely unchanged, maintaining its secondary position, and ground cover vegetation dominated by ferns suffered significant degradation. During the CDO period, the midstorey vegetation was predominantly composed of ferns, with ground cover vegetation taking precedence, midstorey vegetation holding a secondary position, and canopy trees, primarily coniferous, experiencing notable degradation.

(3) SEG analysis indicates that the Santanghu Basin underwent a cyclical evolution from hot and humid to dry and cold, and then back to hot and humid conditions during the early Middle Jurassic (Aalenian–Bajocian). The cooling events observed during this period reflect the basin's response to environmental changes.

Supplementary Materials: The following supporting information can be downloaded at: https://www.mdpi.com/article/10.3390/d16070369/s1, Table S1. Statistics of spores and pollen from the TYY1 Well in the Santanghu Basin, the classification is following Potonié, (1956, 1958).

Author Contributions: B.Y. and J.Y. designed the study. B.Y. and X.Z. identified the sporopollen. B.Y. and J.Y. interpreted data. W.L. and S.S. collected and prepared cores. B.Y. wrote the paper, and all authors contributed to editing the paper. All authors have read and agreed to the published version of the manuscript.

Funding: This research was financially supported by the Collection and Digitization of Physical Geological Data Project, Project Number DD20230138, and the Collection and Interpretation of Important Borehole Core Data from the Physical Geological Database of Tibet Autonomous Region Project, Project Number XZLX-BMC-2023-246.

Institutional Review Board Statement: Not applicable.

Data Availability Statement: The dataset used in this study is available from the first author on reasonable request.

Acknowledgments: We would like to thank the editors and reviewers for their valuable comments on this article.

Conflicts of Interest: Authors declare no conflict of interest.

References

1. Berner, R.A. GEOCARB II: A revised model of atmospheric CO_2 over Phanerozoic time. *Am. J. Sci.* **1994**, *294*, 56–91. [CrossRef]
2. Sellwood, B.W.; Valdes, P.J. Jurassic climates. *Proc. Geol. Assoc.* **2008**, *119*, 5–17. [CrossRef]
3. Jenkyns, H.C. The early Toarcian (Jurassic) anoxic event: Stratigraphic, sedimentary, and geochemical evidence. *Am. J. Sci.* **1988**, *288*, 101–151. [CrossRef]
4. Dera, G.; Brigaud, B.; Monna, F.; Laffont, R.; Pucéat, E.; Deconinck, J.F.; Pellenard, P.; Joachimski, M.M.; Durlet, C. Climatic ups and downs in a disturbed Jurassic world. *Geology* **2011**, *39*, 215–218. [CrossRef]
5. Deng, S.H.; Lu, Y.Z.; Zhao, Y.; Fan, R.; Yang, X.J.; Li, X.; Sun, B.N. The Jurassic palaeoclimate regionalization and evolution of China. *Earth Sci. Front.* **2017**, *24*, 107–142.
6. Dera, G.; Pellenard, P.; Niege, P.; Deconinck, J.F.; Pucéat, E.; Dommergues, J.L. Distribution of clay minerals in Early Jurassic peritethyan seas: Palaeoclimatic significance inferred from multiproxy comparisons. *Palaeogeogr. Palaeoclimatol. Palaeoecol.* **2009**, *271*, 39–51. [CrossRef]
7. Korte, C.; Hesselbo, S.P. Shallow marine carbon and oxygen isotope and elemental records indicate icehouse-greenhouse cycles during the Early Jurassic. *Paleoceanography* **2011**, *26*, PA4219. [CrossRef]
8. Zhang, L.W.; Yan, D.T.; Yang, S.G.; Li, B.Q.; Fu, H.J.; Wang, G.; Yang, X.R.; Zhang, W.L.; Zhang, J.F. Evolution of the Middle Jurassic paleoclimate: Sedimentary evidence from coal-bearing strata in the Santanghu Basin, NW China. *J. Asian Earth Sci.* **2023**, *242*, 105495. [CrossRef]
9. Suchéras-Marx, B.; Giraud, F.; Fernandez, V.; Pittet, B.; Lécuyer, C.; Olivero, D.; Mattioli, E. Duration of the Early Bajocian and the associated $\delta^{13}C$ positive excursion based on cyclostratigraphy. *J. Geol. Soc.* **2013**, *170*, 107–118. [CrossRef]
10. Suchéras-Marx, B.; Suan, G.; Giraud, F.; Mattioli, E.; Khozyem, H.M.; Mazur, J.-C.; Fantasia, A.; Spangenberg, J.E.; Adatte, T. New insights into the early Bajocian (Middle Jurassic) carbon cycle perturbation. *Sedimentologika* **2023**, *1*, 1–18. [CrossRef]
11. Price, G.D. Carbon-isotope stratigraphy and temperature change during the Early–Middle Jurassic (Toarcian–Aalenian), Raasay, Scotland, UK. *Palaeogeogr. Palaeoclimatol. Palaeoecol.* **2009**, *285*, 255–263. [CrossRef]
12. Dai, X.; Du, Y.; Ziegler, M.; Wang, C.; Ma, Q.; Chai, R.; Guo, H. Middle Triassic to Late Jurassic climate change on the northern margin of the South China Plate: Insights from chemical weathering indices and clay mineralogy. *Palaeogeogr. Palaeoclimatol. Palaeoecol.* **2022**, *585*, 110744. [CrossRef]
13. Sun, L.X.; Zhang, Y.; Zhang, T.F.; Cheng, Y.H.; Li, Y.F.; Ma, H.L.; Yang, C.; Guo, J.C.; Lu, C.; Zhou, X.G. Jurassic sporopollen of Yan'an formation and Zhiluo formation in the northeastern Ordos basin, Inner Mongolia, and its paleoclimatic significance. *Earth Sci. Front.* **2017**, *24*, 32–51.
14. Zhang, H.Q.; Wang, T.D.; Yan, C.F.; Yuan, J.Y. The subdivision and correlation of the Jurassic system of the Minhe basin. *J. Stratigr.* **2007**, *31*, 62–67.
15. Wang, Y.D.; Jiang, D.X.; Yang, H.Q.; Sun, F. Middle Jurassic palynoflora and its palaeoenvironmental implication in Turpan depression, Xinjiang. *Acta Sedimentol. Sin.* **1997**, *15*, 133–140.
16. Liu, Z.S.; He, Z.S.; Dong, K.L. Palynological assemblage of an adrilling-section (basal part of the Kizilnur formation) from Yaha, Kuqa, Xinjiang, N W China. *Acta Micropalaeontol. Sin.* **1999**, *16*, 82–88.
17. Wei, Y.; Yang, B.; Xia, H.D.; Deng, H.J. Paleovegetation and paleoclimate during Mid-Late Eocene in Fushun basin. *Earth Sci.* **2021**, *46*, 1848–1861.
18. Guiot, J.; Pons, A.; de Beaulieu, L.; Reille, M. A 140000 year continental climate reconstruction from two European pollen records. *Nature* **1989**, *338*, 309–313. [CrossRef]
19. Li, B.; Wen, X.F.; Zhao, B.; Qiu, H.T.; Wang, X.Q.; Pei, Z.C. Sporo-pollen assemblages and paleoclimate analysis since the Late Pleistocene sediments of Nanyang basin. *Geol. Sci. Technol. Inf.* **2015**, *34*, 49–56.
20. Birks, H.J.B.; Birks, H.H.; Ammann, B. The fourth dimension of vegetation. *Science* **2016**, *354*, 412–413. [CrossRef] [PubMed]
21. Zhang, K. The characteristic of plate tectonic evolution and the evaluation of hydrocarbon prospect of Santanghu basin, Xinjiang. *Xinjiang Pet. Geol.* **1993**, *14*, 1–13.
22. Pan, Y.S.; Huang, Z.L.; Li, T.J.; Guo, X.B.; Xu, X.F.; Chen, X. Environmental response to volcanic activity and its effect on organic matter enrichment in the Permian Lucaogou formation of the Malang Sag, Santanghu basin, Northwest China. *Palaeogeogr. Palaeoclimatol. Palaeoecol.* **2020**, *560*, 110024. [CrossRef]
23. Grimm, E.C. CONISS: A FORTRAN 77 program for stratigraphically constrained cluster analysis by the method of incremental sum of squares. *Comput. Geosci.* **1987**, *13*, 13–35. [CrossRef]
24. Grimm, E.C. *Tilia, TiliaGraph and TGView Software*; Illinois State Museum: Springfield, IL, USA, 2001.
25. Abbink, O.A.; Van Konijnenburg-Van Cittert, J.H.A.; Visscher, H. A sporomorph ecogroup model for the Northwest European Jurassic—Lower Cretaceousi: Concepts and framework. *Neth. J. Geosci. Geol. Mijnb.* **2004**, *83*, 17–31. [CrossRef]
26. Li, L.Q.; Wang, Y.D.; Liu, Z.S.; Zhou, N.; Wang, Y. Late Triassic palaeoclimate and palaeoecosystem variations inferred by palynological record in the northeastern Sichuan Basin, China. *Paläontol. Z.* **2016**, *90*, 327–348. [CrossRef]

27. Li, L.Q.; Wang, Y.D.; Vajda, V.; Liu, Z.S. Late Triassic ecosystem variations inferred by palynological records from Hechuan, southern Sichuan Basin, China. *Geol. Mag.* **2018**, *155*, 1793–1810. [CrossRef]
28. Kershaw, P.; Wagstaff, B. The southern conifer family Araucariaceae: History, status, and value for paleoenvironmental reconstruction. *Annu. Rev. Ecol. Syst.* **2001**, *32*, 397–414. [CrossRef]
29. Couper, R.A. British Mesozoic microspores and pollen grains. A systematic and stratigraphic study. *Palaeontogr. Abt. B Palaeophytol. Palaeobot.-Palaeophytol.* **1958**, *103*, 75–179.
30. Huang, L.; Zhang, X.J.; Li, G.Z.; Ji, X.K.; Han, X.; Wang, Z.Y.; Liu, Z.Q.; Hou, Z.M.; Ai, Z.H. Sporopollen assemblage from the Middle Jurassic of the northeastern Ordos Basin, Inner Mongolia, and their paleoclimatic implications. *Acta Geol. Sin.* **2023**, *97*, 1390–1406.
31. Liu, Z.S. Early and middle Jurassic sporo-pollen assemblages from the Shiguai coal-field of Baotou, Nei Monggol. *Acta Palaeontol. Sin.* **1982**, *21*, 371–381.
32. Du, B.A.; Li, X.R.; Duan, W.H. Sporo-pollen assemblages from Yan'an and Zhiluo formation in Chongxin county, Gansu province. *Acta Micropalaeontol. Sin.* **1982**, *21*, 597–609.
33. Huang, P. Early-middle Jurassic sporopollen assemblages from Dananhu coalfield of Thuha basin, Xinjiang and their stratigraphical significance. *Acta Palaeontol. Sin.* **1995**, *34*, 171–197.
34. Wang, Y.D.; Jiang, D.X.; Yang, H.Q.; Sun, F. Middle Jurassic spore-pollen assemblages from Turpan-Shanshan area, Xinjiang. *Acta Bot. Sin.* **1998**, *40*, 969–976.
35. Qian, L.J.; Wang, J.G. *Peat-Forming Materials and Swampy Environment of Middle Jurassic Terrestrial Bituminite*; China Coal Industry Publishing House: Beijing, China, 1994; pp. 1–139.
36. Liu, Z.S.; Zhang, Z.H. Late Early Jurassic Fuxian Formation spore pollen assemblage and its significance, Fuxian county, Shaanxi. In *International Symposium on Geological Sciences at Peking University*; Seismological Press: Beijing, China, 1998; pp. 430–438.
37. Xu, Y.L.; Zhang, W.P. *Mesozoic Strata and Paleontologyinthe Shaanxi-Gansu-Ningxia Basin (Volume I)*; Geological Publishing House: Beijing, China, 1980; pp. 143–186.
38. Liu, Z.S. Sporo-pollen assemblage from middle Jurassic Xishanyao formation of Shawan, Xinjiang, China. *Acta Palaeontol. Sin.* **1990**, *29*, 63–87.
39. Santos, A.A.; Wang, X.; Qiang, F.Q.; Diez, J.B. First palynological data from the Jurassic South Xiangshan Formation (Nanjing area, China). *Geobios* **2018**, *51*, 559–570. [CrossRef]
40. Huang, P.; Li, J.G. Sporopollen assemblages from the Xishanyao and Toutunhe formation at the Honggou Section of the Manasi River, Xinjiang and their stratigraphical significance. *Acta Micropalaeontol. Sin.* **2007**, *24*, 170–193.
41. Ilyina, V.I. Subdivision and correlation of the marine and non-marine Jurassic sediments in Siberia based on palynological evidence. *Rev. Palaeobot. Palynol.* **1986**, *48*, 357–364. [CrossRef]
42. Huang, P. Middle Jurassic sporopollen assemblages from Tangqiang-3 well of Santanghu basin, Xinjiang. *Acta Micropalaeontol. Sin.* **2002**, *19*, 178–192.
43. Sun, G.; Miao, Y.Y.; Mosbrugger, V.; Ashraf, A.R. The Upper Triassic to Middle Jurassic strata and floras of the Junggar Basin, Xinjiang, Northwest China. *Palaeobiodivers. Palaeoenviron.* **2010**, *90*, 203–214. [CrossRef]
44. Korte, C.; Hesselbo, S.P.; Ullmann, C.V.; Dietl, G.; Ruhl, M.; Schweigert, G.; Thibault, N. Jurassic climate mode governed by ocean gateway. *Nat. Commun.* **2015**, *6*, 10015. [CrossRef]
45. Jones, C.E.; Jenkyns, H.C.; Coe, A.L.; Stephen, H.P. Strontium isotopic variations in Jurassic and Cretaceous seawater. *Geochim. Cosmochim. Acta* **1994**, *58*, 3061–3074. [CrossRef]
46. Ferreira, J.; Mattioli, E.; Sucherás-Marx, B.; Giraud, F.; Duarte, L.V.; Pittet, B.; Suan, G.; Hassler, A.; Spangenberg, J.E. Western Tethys Early and Middle Jurassic calcareous nannofossil biostratigraphy. *Earth-Sci. Rev.* **2019**, *197*, 102908. [CrossRef]
47. Bodin, S.; Mau, M.; Sadki, D.; Danisch, J.; Nutz, A.; Krencker, F.-N.; Kabiri, L. Transient and secular changes in global carbon cycling during the early Bajocian event: Evidence for Jurassic cool climate episodes. *Glob. Planet. Change* **2020**, *194*, 103287. [CrossRef]
48. Shen, J.; Yu, J.X.; Chen, J.B.; Algeo, T.J.; Xu, G.Z.; Feng, Q.L.; Shi, X.; Planavsky, N.J.; Shu, W.C.; Xie, S.C. Mercury evidence of intense volcanic effects on land during the Permian-Triassic transition. *Geology* **2019**, *47*, 1117–1121. [CrossRef]
49. Yang, B.; Zhang, X.Z.; Yi, J.J.; Shi, W.X.; Sun, S.Y.; Sun, S.Y.; Su, G.F. Carbon-cycle perturbations and intensified continental chemical weathering linked to volcanism during the Jenkyns Event in the Ordos Basin. *Geol. J.* **2024**, *59*, 1298–1321. [CrossRef]

Disclaimer/Publisher's Note: The statements, opinions and data contained in all publications are solely those of the individual author(s) and contributor(s) and not of MDPI and/or the editor(s). MDPI and/or the editor(s) disclaim responsibility for any injury to people or property resulting from any ideas, methods, instructions or products referred to in the content.